

LOSS ANALYSIS AND IMPROVEMENTS OF INDUSTRIALLY FABRICATED CZ-SI SOLAR CELLS BY MEANS OF PROCESS AND DEVICE SIMULATIONS

SUMMARY

We model Cz cells, fabricated in a pilot line, with a combination of process, device and circuit simulations. This allows us to separate the various resistive losses and to determine the recombination losses contributed from various device components. Such data are vital for identifying performance improvement strategies. As the model is based on currently fabricated cells, it gives precise predictions for specific cell improvements and the associated thermal budgets. We forecast the extent to which the emitter needs to be improved until the recombination losses in the boron-doped Cz base dominate. At that point, the cell reaches an efficiency of 18.9% after degradation. To increase the efficiency beyond about 19.4% after degradation, the boron-doped Cz material needs to be improved.

1. INTRODUCTION

In the IC industry, numerical process and device modeling are well established tools for accelerating device development. The PV industry has also started to employ such modeling for developing advanced device architectures such as selective emitters and improved rear surfaces.

To make reliable predictions, the models need to be tested and calibrated based on fabricated solar cells. Over the last decades, several models have been developed specifically for PV applications, see [1-6] for examples. Because solar cells are large-area diodes, a combination of device and circuit modeling was shown to account for all relevant losses [7]. We show how such models can be used to accelerate the development of improved cells.

2. LOSS ANALYSIS

2.1. Resistive losses

As a first step, it is important to separate carefully resistive and recombination losses, because their optimization strategies differ greatly. As both these losses influence the IV curve, separating them is a rather delicate task. From the IV curves, the lumped series resistance $R_s(V)$ is commonly extracted as a function of voltage V in two different ways (see e.g. [8]): either by comparing the 1-sun IV curve with the $J_{sc}V_{oc}$ curve, or by comparing two illuminated IV curves at slightly different light intensities. Figure 1 shows that the $J_{sc}V_{oc}$ method underestimates R_s at low V due to the injection-dependent SRH lifetime in Cz material (see below). At MPP, $0.72 \Omega\text{cm}^2$ is extracted instead of $0.84 \Omega\text{cm}^2$ obtained using the double light-level (dll) method. The difference between the simulated internal and the lumped resistance in Fig. 1 arises due to losses in the front metallization.

2.2. Recombination losses

Knowing the contribution of the recombination losses from various device parts is vital for improvement strategies. Nevertheless, many institutions and companies do not accurately know the limiting losses of their cells. We express the losses as recombination currents $qR(V)$, as shown in Fig. 2, where R is the recombination rate and q the unit charge.

Three main features become apparent: (i) the emitter losses dominate the overall losses, (ii) shortly followed by the SRH losses in the Cz base material, which (iii) increase sub-exponentially between V_{mpp} and V_{oc} . The reason for (iii) is that the excess carrier lifetime in boron-doped Cz material strongly improves with higher injection levels [4,5], i.e. toward

higher voltages. This has important consequences on the optimization as explained below.

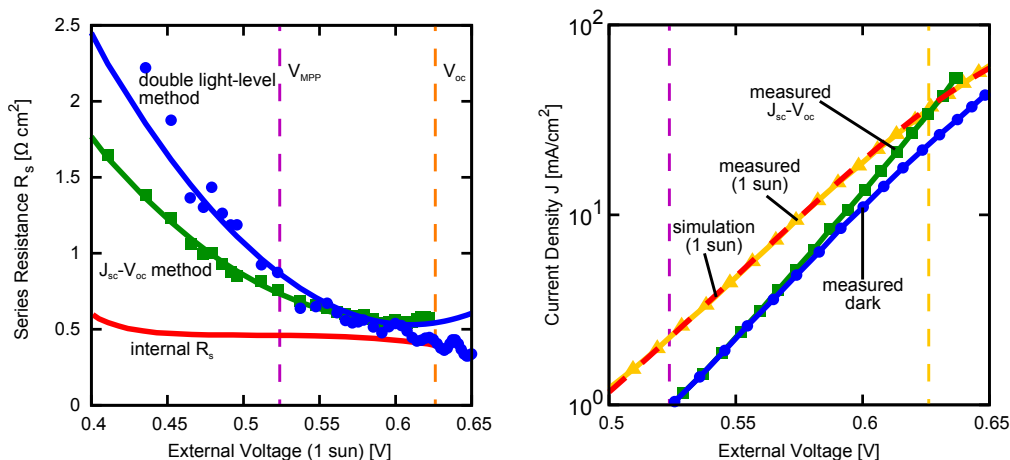


Fig. 1 Left: The lumped series resistance extracted from the 1-sun IV and the J_{sc} - V_{oc} . Right: the experimental and simulated IV curves.

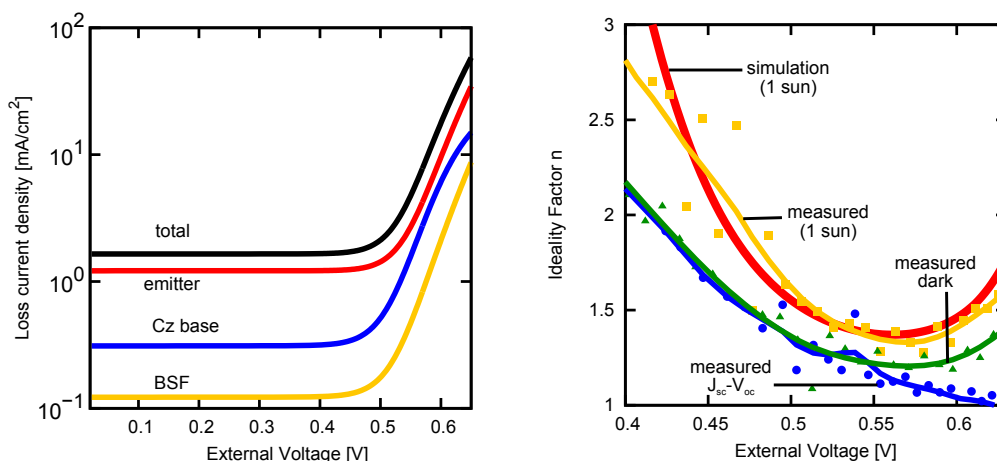


Fig. 2 Left: The simulated recombination losses in various device regions. Right: The ideality factor curves (symbols/lines: experiment, thick red line: simulation).

3. PREDICTION OF EFFECTS OF DESIGN CHANGES

3.1. Improvement of the emitter

Figure 3 shows a process simulation of our emitter diffusion by means of the 3-stream coupled diffusion model [9]. Because there is no model available for the phosphosilicate glass (PSG), the peak dopant density must be assumed. This inhibits a proper prediction of process changes. Therefore, we develop a PV-specific model for the PSG layer. By combining this improved process model with device and circuit simulations, we predict the minimal thermal budget required for fabricating a nitride-passivated emitter that is just good enough so the cell efficiency is limited by recombination in the base. Additionally, this emitter is compatible with the minimum finger distance and minimum finger width attainable by screen printing. The dashed curve in Figure 3 shows an example.

3.2. Potential cell efficiency

As discussed in Fig. 2, the recombination losses in the Cz base increase sub-exponentially with V due to the injection-dependent excess carrier lifetime. Therefore, an improvement of the emitter to the extent that the losses in the base dominate the overall

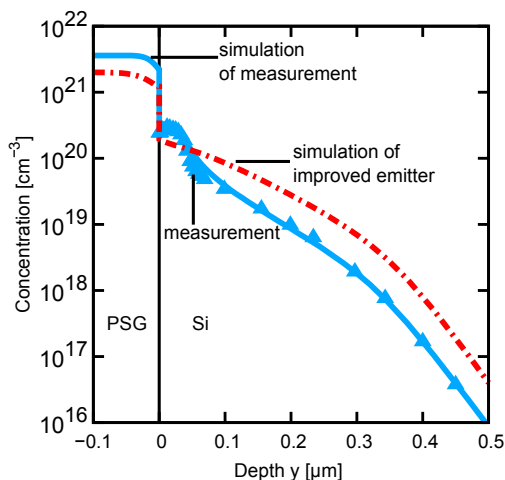


Fig. 3 The phosphorus dopant profile, measured by ECV (symbols) and simulated (line). Process simulation of an improved emitter is shown by the dashed line.

losses, leads to a bent IV curve and, accordingly, to a reduced fill factor (FF). This reduction in FF is not due to resistive losses, but due to recombination saturation effects in the base. This becomes obvious when the resistive losses are carefully separated from the recombination losses, as described above. This saturation effect increases with the wafer resistivity, and hampers efforts to reach efficiency levels higher than about 19.4% after degradation for standard CZ material.

Tab. 1 Comparison of measured and simulated cell parameters.

	J_{sc}	V_{oc}	J_{mpp}	V_{mpp}	Eff
Experiment: before degradation	36.6	627.8	34.31	527.3	18.09
Experiment: after degradation	36.2	626.1	33.88	523.8	17.75
Simulation: as is	36.2	625.8	33.78	525.4	17.75
Simulation improved emitter, same fingers	37.41	644.8	34.95	540.1	18.88

- [1] P.P. Altermatt, A. Schenk, F. Geelhaar, and G. Heiser, "Reassessment of the intrinsic carrier density in crystalline silicon in view of band-gap narrowing", *Journal of Applied Physics* 93, 1598 (2003).
- [2] P.P. Altermatt, J.O. Schumacher, A. Cuevas, M. J. Kerr, S.W. Glunz, R.R. King, and G. Heiser, "Numerical modeling of highly doped Si:P emitters based on Fermi-Dirac statistics and self-consistent material parameters", *Journal of Applied Physics* 92, 3187 (2002).
- [3] M. J. Kerr and A. Cuevas, "General parameterization of Auger recombination in crystalline silicon", *Journal of Applied Physics* 91, 2473 (2002).
- [4] K. Bothe, R. Sinton, J. Schmidt, "Fundamental Boron-Oxygen-related Carrier Lifetime Limit in Mono- and Multicrystalline Silicon", *Progress in PV* 13, 287 (2005).
- [5] S. Rein and S. W. Glunz, "Electronic properties of the metastable defect in boron-doped Czochralski silicon: Unambiguous determination by advanced lifetime spectroscopy", *Journal of Applied Physics* 82, 1054 (2003).
- [6] R. Bock, P.P. Altermatt, J. Schmidt, and R. Brendel, "Formation of aluminum-oxygen complexes in highly aluminum-doped silicon", *Semiconductor Science and Technology* 25, 105007 (2010).
- [7] P.P. Altermatt, G. Heiser, A.G. Aberle, A. Wang, J. Zhao, S.J. Robinson, S. Bowden, and M.A. Green, "Spatially resolved analysis and minimization of resistive losses in high-efficiency Si solar cells", *Progress in PV* 4, 399 (1996).
- [8] A.G. Aberle, S.R. Wenham, and M.A. Green, "A new method for accurate measurements of the lumped series resistance of solar cells", 23th IEEE Specialists Conf, Louisville, USA, 1993, p. 133.
- [9] S.T. Dunham, "A quantitative model for the coupled diffusion of phosphorus and point defects in silicon", *Journal of the Electrochemical Society* 139, 2628 (1992).